Gating of the expressed $Ca_v3.1$ calcium channel

L'. Lacinová[a,b,*], N. Klugbauer[b], F. Hofmann[b]

[a] *Institute of Molecular Physiology and Genetics, Slovak Academy of Sciences, Vlárska 5, 833 04 Bratislava, Slovak Republic*
[b] *Institut für Pharmakologie und Toxikologie der Technischen Universität München, Biedersteiner Str. 29, 80802 München, Germany*

Received 26 August 2002; revised 18 September 2002; accepted 27 September 2002

First published online 9 October 2002

Edited by Maurice Montal

Abstract Intramembrane charge movement originating from $Ca_v3.1$ (T-type) channel expressed in HEK 293 cells was investigated. Ion current was blocked by 1 mM La^{3+}. Charge movement was detectable for depolarizations above ~−70 mV and saturated above +60 mV. The voltage dependence of charge movement followed a single Boltzmann function with half-maximal activation voltage +12.9 mV and +12.3 mV and with slopes of 22.4 mV and 18.1 mV for the ON- and OFF-charge movement, respectively. Inactivation of I_{Ca} by prolonged depolarization pulse did not immobilize intramembrane charge movement in the $Ca_v3.1$ channel.

Key words: $Ca_v3.1$ channel; Charge movement; Low-voltage activated calcium channel; Channel gating

1. Introduction

Voltage-operated Ca^{2+} channels consist of four repeats each containing the six transmembrane segments S1–S6 [1]. The S4 segment contains five to six positive charged amino acids. Voltage-dependent opening and closing of these ion channels are accompanied by movements of the S4 segment in outward or inward direction, respectively [2]. Because of its electrical charge movement of this segment causes measurable current known as gating current or non-linear charge movement [3,4]. Transition of channels into the inactivated state may be associated with partial immobilization of the gating charge, as shown for Na^+ channel [5,6].

Gating current arising from the activation of high-voltage activated (HVA) calcium channels was measured previously both from acutely isolated neuronal [7], cardiac [8,9] or skeletal [10,11] muscle cells and from heterologously expressed L-type $Ca_v1.2$ calcium channels [12,13,14] and non-L-type $Ca_v2.2$ [15,16,17] and $Ca_v2.3$ [18,19,20] calcium channels. A major obstacle to analysis of gating currents from low-voltage activated (LVA) T-type calcium channels is their low expression level in native tissues [21], which results in charge movement too small to be detected. Cloning of $Ca_v3.n$ channel family [22] enabled high expression of these channels in heterologous expression system and consequently also analysis of gating currents reflecting their activation. Here we report measurements of charge movement from HEK 293 cells expressing neuronal T-type $Ca_v3.1$ calcium channel.

2. Materials and methods

HEK 293 cells were transiently transfected with DNA encoding for $Ca_v3.1$ [23] using Lipofectamine (Gibco).

Bath solution contained (in mM): NMDG 140, HEPES 10, $CaCl_2$ 2, $MgCl_2$ 2; pH 7.4 with HCl. Pipette solution contained (in mM): CsCl 130, MgATP 5, EGTA 10, HEPES 10; pH 7.4 with CsOH. Osmolarity of internal solutions was measured (typical value approximately 300 mOsm) and osmolarity of external solution was adjusted by adding glucose to the value by 2–3 mOsm lower.

Whole cell currents were measured using EPC 9 patch clamp amplifier (HEKA Elektronik, Lambrecht, Germany). Patch pipette were pulled from borosilicate glass and when filled with pipette solution, their input resistance was between 1.8 and 2.0 MΩ. Typical cell size was between 20 and 40 pF. Access resistance was between 3.0 and 4.0 MΩ and was compensated up to 70%. Data were recorded with HEKA Pulse 8.30 software package and analyzed with HEKA Pulse 8.30 software and with Origin 6.1 software (OriginLab Co., Northampton, MA, USA). Symmetrical capacity transients and linear leakage current were subtracted by P/-8 procedure. To maximize signal/noise ratio, for analysis of gating currents three consecutively recorded traces activated by identical voltage protocol were averaged.

Holding potential (HP) was −100 mV in all experiments. Gating currents were measured by 15 ms long depolarizations to membrane potentials (V) between −90 mV and +80 mV. Asymmetrical charge movement was evaluated by integrating the area below charge transients observed at the beginning and after the end of each depolarizing pulse. For each investigated cell Q_{on}–V and Q_{off}–V relationships were normalized to maximal Q_{on} or Q_{off}, respectively. Normalized Q-V curves were averaged across the cells. Charge–voltage relationships were fitted by Boltzmann equation:

$$Q(V)/Q_{max} = 1/(1 + \exp\,(V - V_{0.5})/dV)$$

where $V_{0.5}$ is membrane voltage at which half-maximal charge activation is reached, $Q(V)$ represents charge measured at the test membrane voltage V, Q_{max} is maximal observed charge and dV is slope factor.

Voltage dependence of current activation was evaluated from tail current amplitudes. Normalized amplitudes were averaged across cells and fitted by double Boltzmann distribution:

$$I(V)/I_{max} = (I_1/I_{max})/(1 + \exp\,(V - V_{1half})/dV1) +$$

$$(I_2/I_{max})/(1 + \exp\,(V - V_{2half})/dV2)$$

where $I(V)$ is amplitude of tail current measured at membrane potential V, I_{max} is the maximal tail current amplitude, I_1 and I_2, V_{1half} and V_{2half}, $dV1$ and $dV2$ are relative amplitudes, half-maximal activation voltages and slopes of voltage dependencies of the first and the second components of current activation.

3. Results

3.1. Gating current measurement of $Ca_v3.1$ channel

In order to measure gating, ion current flowing through the channel must be blocked. Previously, we have shown that the

*Corresponding author. Fax: (421)-2-5477 3666.
E-mail address: umfglaci@kramare.savba.sk (L. Lacinová).

0014-5793/02/$22.00 © 2002 Published by Elsevier Science B.V. on behalf of the Federation of European Biochemical Societies.
PII: S0014-5793(02)03509-3

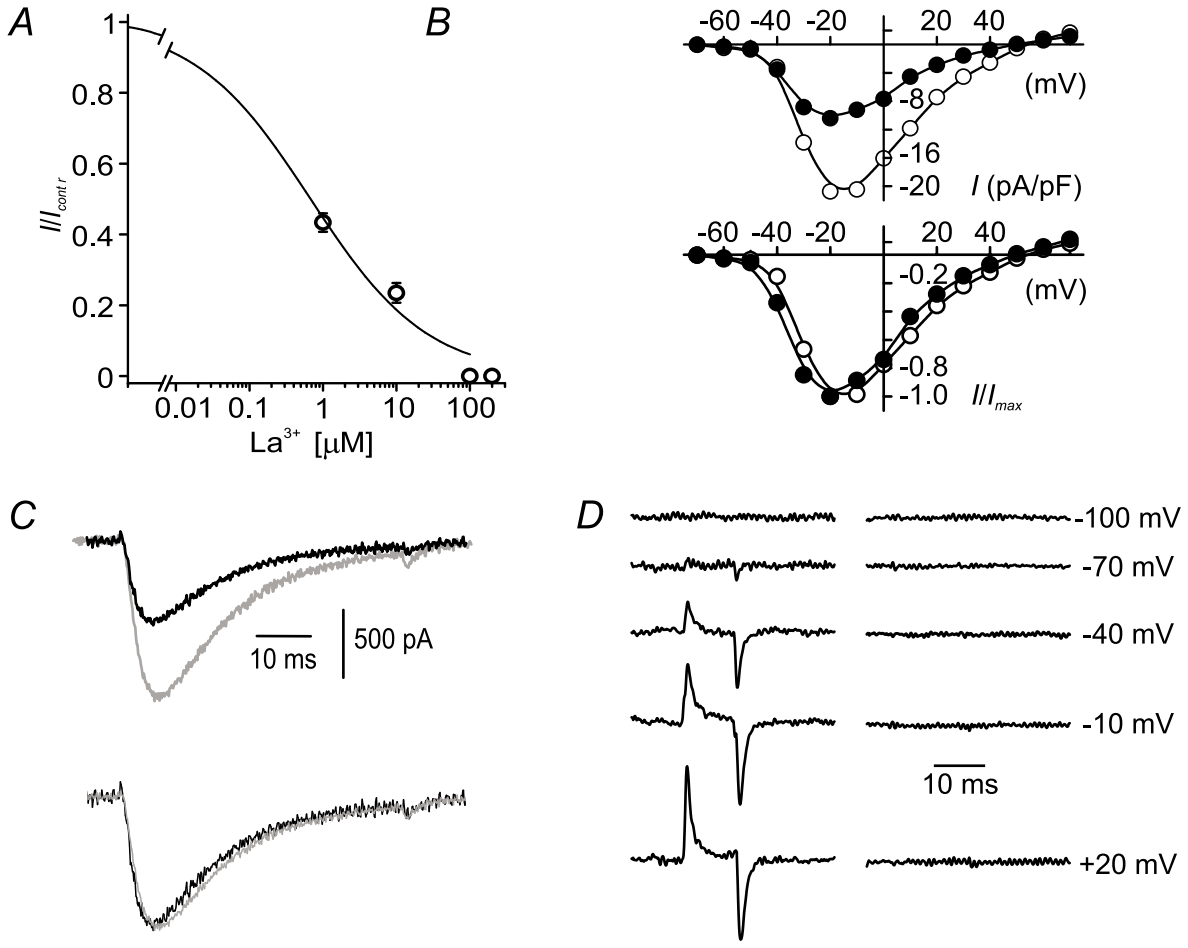

Fig. 1. Block of inward calcium current through expressed $Ca_v3.1$ channel by La^{3+}. A: Dose-dependence of the inhibition of I_{Ca} carried by 2 mM Ca^{2+} through expressed $Ca_v3.1$ channel. Current was measured during 40 ms long depolarizing pulses from the HP of −100 mV to −20 mV at a frequency of 0.2 Hz. The data were fitted by the Hill equation with a coefficient of 1 resulting in an IC_{50} of 0.7 μM. Four to 11 individual measurements were averaged for each point. B: An example of current–voltage relationship measured from a cell expressing $Ca_v3.1$ channel in the absence (○) and presence (●) of 1 μM of La^{3+}. Upper panel shows raw data, which are normalized to the maximal current in lower panel to facilitate comparison. C: Examples of current traces measured in the absence (gray) and presence (black) of 1 μM of La^{3+}. Same cell as in a panel (B). Upper panel shows raw traces, which are normalized to the same amplitude in lower panel to facilitate comparison. D: Examples of current traces measured during 10 ms long depolarizing pulses from the HP of −100 mV to voltages marked next to each trace in the presence of 1 mM La^{3+}. Individual traces were recorded from a cell expressing $Ca_v3.1$ channel (left) or from a cell in which no channel activity was detected in the absence of La^{3+} ions (right).

divalent ions Cd^{2+} and Ni^{2+} alter activation and deactivation kinetics as well as the voltage dependence of the current through expressed $Ca_v3.1$ channel [24]. Therefore, we tested suitability of the trivalent cation La^{3+}. 1 μM La^{3+}, the concentration which blocks about 50% of inward current carried by 2 mM Ca^{2+} (Fig. 1A), had only negligible effect on the shape of the current–voltage relationship (Fig. 1B) and current kinetics (Fig. 1C).

Charge movement was consistently observed in cells with current amplitude 1 nA or bigger. In these cells, the gating current was first detectable at depolarizations to membrane voltage between −70 and −60 mV (Fig. 1D). When the maximal current amplitude was below 1 nA, the threshold for detection of gating was at membrane potential ∼−30 mV to −20 mV. These cells were not included into the further analysis. Charge movements were not detectable in HEK 293 cells that were transfected by an empty vector or non-transfected. These cells showed capacity transient that were eliminated completely by the P/-8 procedure (Fig. 1D).

3.2. Voltage dependence of channel activation and charge movement of the $Ca_v3.1$ channel

Steady state activation of calcium current could be evaluated from peak tail current amplitude measured at constant repolarization potential after test pulses of varying amplitudes and lengths [25,26]. To circumvent a decrease of tail amplitude due to channel inactivation during depolarizing pulse [23], the length of the depolarizing pulse was adjusted to the time to peak at each pulse amplitude. Pulse length was 15 ms for depolarizations between −90 and −50 mV, then decreased continually to 2 ms at +30 mV and remained constant for higher depolarizations (Fig. 2A). Tail amplitudes measured at the end of each pulse (Fig. 2B) were normalized to the maximal tail amplitude, averaged and fitted by Boltzmann function (Fig. 2C). Fit of experimental data by single Boltzmann distribution did not produce satisfactorily results. The current–voltage relationship could be fitted optimal only with two independent functions. We have analyzed the significance of fit improvement by Fischer's test. Difference between fits by

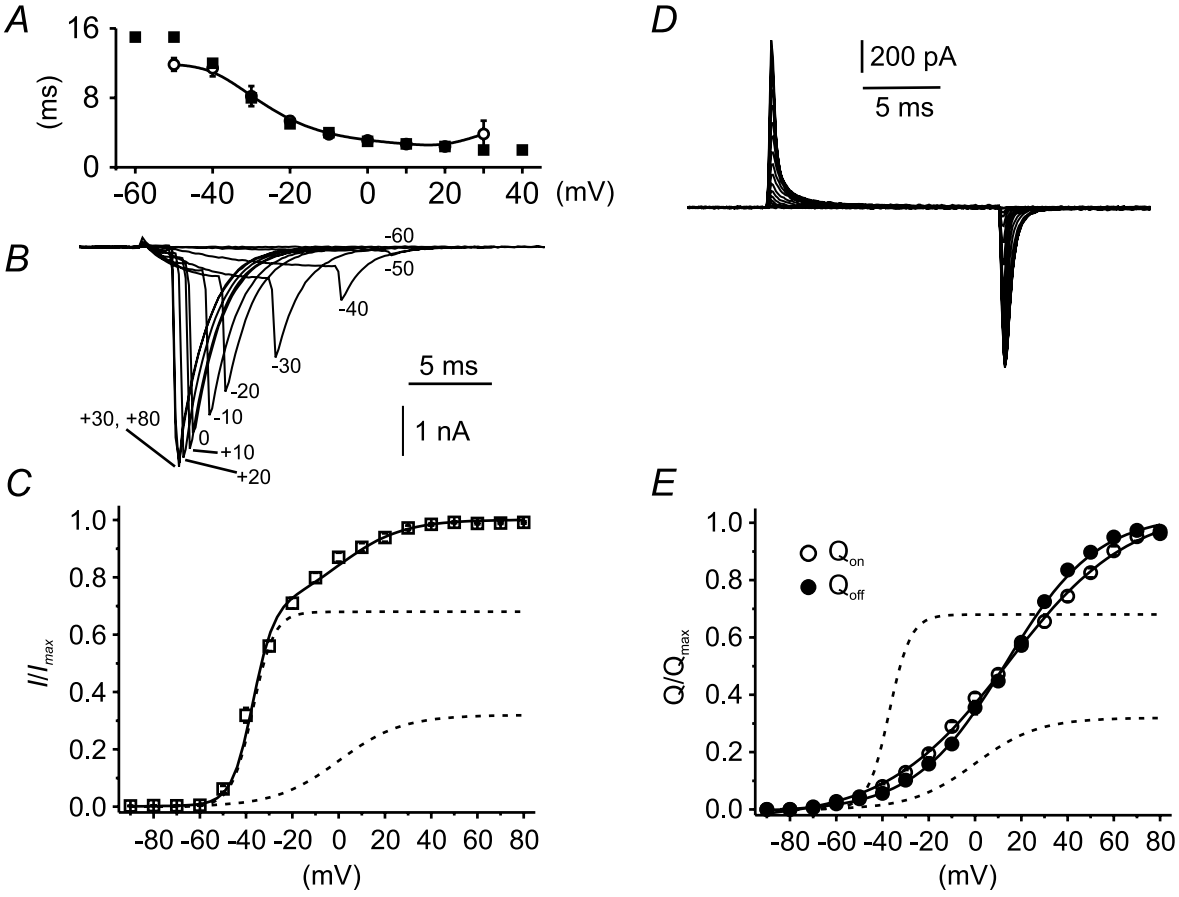

Fig. 2. Voltage dependence of ionic and gating currents activation of $Ca_v3.1$ channel. A: Activation of ionic current was evaluated from the amplitudes of tail currents measured at constant repolarizing potential of −100 mV after depolarizations to potentials between −90 and +80 mV. The length of the depolarizing pulse was adjusted according to time-to-peak of the inward current observed at each potential. (■) – measured time to peak, (○) – pulse length used in the experimental protocol. B: An example of tail currents measured according to the protocol described in panel A. Depolarization potentials are marked next to each trace. C: Normalized amplitudes of tail currents obtained from the protocol described in panel A ($n=11$, □). Solid line represents fit of experimental points by double Boltzmann distribution whose individual components are demonstrated by dashed lines. Relative amplitudes of both components were 68% and 32%, half-activation voltages were −37.1 mV and 0.0 mV and slopes were 4.5 mV and 13.7 mV. D: Families of gating currents measured from a cell expressing $Ca_v3.1$ channel in the presence of 1 mM La^{3+}. E: Total charge moved during each pulse was calculated by integrating the area under the gating current records. Individual measurements were normalized and averaged. (○) – Q_{on}, (●) – Q_{off}. Solid lines represent Boltzmann functions fitted to the experimental points. Half-maximal activation voltages were +12.9 mV and +12.3 mV and slopes were 22.4 mV and 18.1 mV for Q_{on} and Q_{off}, respectively. Dashed lines demonstrate two components of current activation evaluated from the data presented in panel C.

single and double Boltzmann distribution was significant on 0.001 level. The first component of the current activation contributed 68% to the total activation, had a steep slope of 4.5 ± 0.4 mV ($n=11$) and half-maximal activation voltage of −37.1 ± 0.7 mV. The second component contributed 32% to the total amount of activated channels, had shallow slope of 13.7 ± 0.8 mV and a half-maximal activation voltage of 0.0 ± 3.8 mV. Both components are demonstrated separately by dashed lines in Fig. 2C. Asymmetrical charge movements were measured by a series of depolarizing pulses to the voltages between −90 and +80 mV (Fig. 2D). The length of the pulse was 15 ms to allow complete decay of ON-charge movement. Total charge moved by each depolarization was evaluated by integrating the area below the charge transients observed at the beginning and after the end of the test pulse. These amplitudes were plotted against the pulse potential (Fig. 2E). Both voltage dependencies followed a single Boltzmann function with half-maximal activation voltage of +12.9 ± 1.4 mV ($n=25$) and +12.3 ± 0.7 mV and with a slope of 22.4 ± 0.4 mV and 18.1 ± 0.4 mV for the ON- and OFF-charge movement, respectively. The slopes were significantly different (paired Student's t-test). The start of both Q_{on} and Q_{off} preceded the start of the fast component of current activation by about 10 mV and the start of slow component of current activation by more than 30 mV (Fig. 2E). The fast component of current activation reached a maximum level positive to −10 mV, when about 30% of the gating charge was transferred.

3.3. Q_{on} and Q_{off} are proportional to maximal current density I_{max}

The amplitudes of Q_{on} and Q_{off} were not significantly different (Fig. 3A). The amount of charge moved by depolarizing pulse was proportional to the number of channels available for activation, i.e. proportional to the current amplitude (Fig. 3B). The average amount of charge moved was

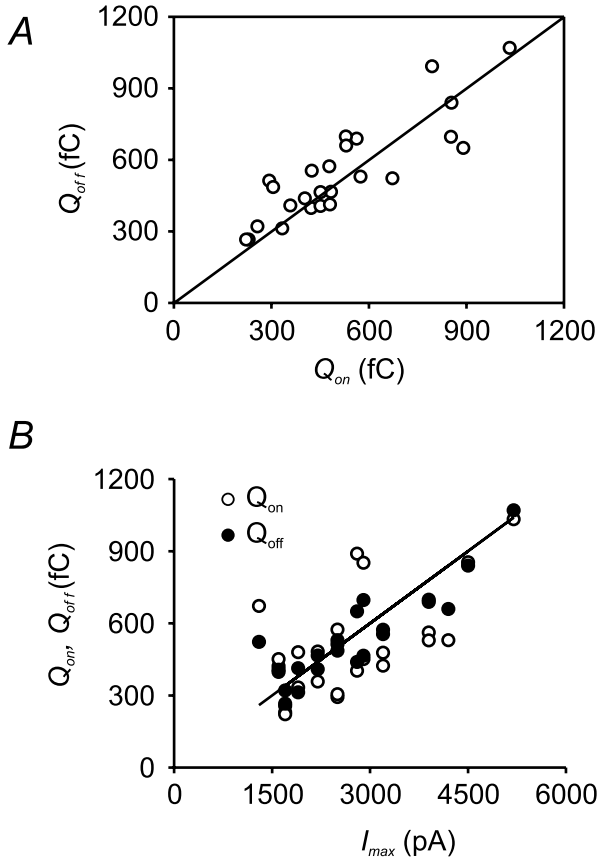

Fig. 3. A: Maximal value of Q_{off} measured for each individual cell was plotted against maximal Q_{on} value from the same cell. Straight line represents unity line. Points above the unity line represent cells in which Q_{off} was bigger than Q_{on}. Points under the unity line represent cells in which Q_{off} was smaller than Q_{on}. Cells with Q_{on} equal Q_{off} lie on the unity line. B: Maximal Q_{on} (○) or Q_{off} (●) values plotted against current amplitude measured at the peak of current–voltage relationship (I_{max}) in the same cell. Straight line has a slope 0.20.

0.20 ± 0.02 fC/pA and 0.20 ± 0.01 fC/pA ($n = 25$) for Q_{on} and Q_{off}, respectively. This proportionality is represented by a straight line with slope of 0.2 in the Fig. 3B.

3.4. OFF-charge movement is not immobilized by prolonged depolarization

Current through $Ca_v3.1$ channel decays rapidly during depolarizing pulse due to transition of the channel from the open into the inactivated and/or closed states. When the length of the depolarizing pulse to −20 mV was gradually prolonged from 10 ms to 55 ms, both current amplitude and tail current amplitude decreased (Fig. 4A). In contrast, the amplitude of Q_{off} remained constant (Fig. 4B,C). The difference between Q_{off} measured after 10 ms long pulse and after 55 ms long pulse was not significant (Student's paired t-test). Unlike in the case of HVA calcium channels, voltage-dependent transition, which causes decay of inward calcium current, does not immobilize gating charge of this LVA channel.

A 55 ms long depolarizing pulse is not sufficient for complete inactivation of $Ca_v3.1$ channel. To reach steady state voltage-dependent inactivation of $Ca_v3.1$ channel, an at least 2 s long depolarizing pulse is necessary [23]. Therefore, we tested the effect of a 5 s long prepulse to 0 mV on the charge movement. As expected, no ON-charge movement was detected after the prepulse. Nevertheless, even 5 s long depolarization did not immobilize the OFF-charge transient (Fig. 4D).

4. Discussion

4.1. The asymmetrical current transients reflect $Ca_v3.1$ channel activity

Several observations provide evidence that the observed current transients reflect $Ca_v3.1$ channel activity and are not contaminated by capacity artefact due to imperfect subtraction procedure and/or movements of charged parts of other channels which may be endogenously expressed in HEK 293 cells. Asymmetrical charge movements were observed exclusively in the cells in which macroscopic $Ca_v3.1$ current was observed. In the cells which underwent the same transfection procedure but did not express measurable calcium current, asymmetric charge movements were not observed. The amplitude of the charge transient was always proportional to the current amplitude. Voltage dependencies of both Q_{on} and Q_{off} were satisfactorily fitted by single Boltzmann distribution. Any contamination by signals of other origins – i.e. distinct from the movement of charged parts of $Ca_v3.1$ channel – would be detected in the absence of expressed $Ca_v3.1$ channels and/or would contribute distinct components to the Boltzmann distribution.

4.2. Gating currents measured from $Ca_v3.1$ differ from gating current measured from HVA calcium channels

Gating currents reported here for LVA $Ca_v3.1$ channels deviate in some aspects from gating currents measured from HVA calcium channels. They precede activation of macroscopic inward current by about 10 mV. This value is smaller than the 30–40 mV difference reported previously for expressed $Ca_v1.2$ channel [27,28] or $Ca_v2.2$ channel [15] but similar to values reported for the expressed $Ca_v2.3$ channel [19,20]. The $Ca_v2.3$ channels have been considered as intermediates between HVA and LVA channels because of their fast kinetics and relatively negative threshold for current activation [1,29,30]. Still, it is possible that 1 mM La^{3+} used in reported experiments caused shift of the voltage dependence of gating current in the positive voltage direction. If this were the case, than the voltage distance between onset of charge movement and ionic current would be more similar to that reported for HVA calcium channels.

Voltage dependencies of gating currents measured from native L-type calcium channels [9] or expressed $Ca_v1.2$ [27], $Ca_v2.2$ [15] and $Ca_v2.3$ channels [18,19] have slopes varying between 15 and 18 mV. The slope reported here for $Ca_v3.1$ channel, i.e. 22.4 mV and 18.1 mV for Q_{on} and Q_{off}, respectively, is slightly higher. Furthermore, in contrast to our finding for $Ca_v3.1$ channels, no difference in slopes was found between Q_{on}–V and Q_{off}–V relationships in HVA calcium channels. While single Boltzmann distribution fits satisfactorily the Q–V relationship of the $Ca_v3.1$ channel, a second component with a slope of 5–8 mV was reported for $Ca_v2.2$ [16] or $Ca_v2.3$ [18] channels. These two components of charge movement correspond to two components of current activation [18]. Similarly to $Ca_v2.3$ current, activation of $Ca_v3.1$ current has two distinct components with distinct slopes and

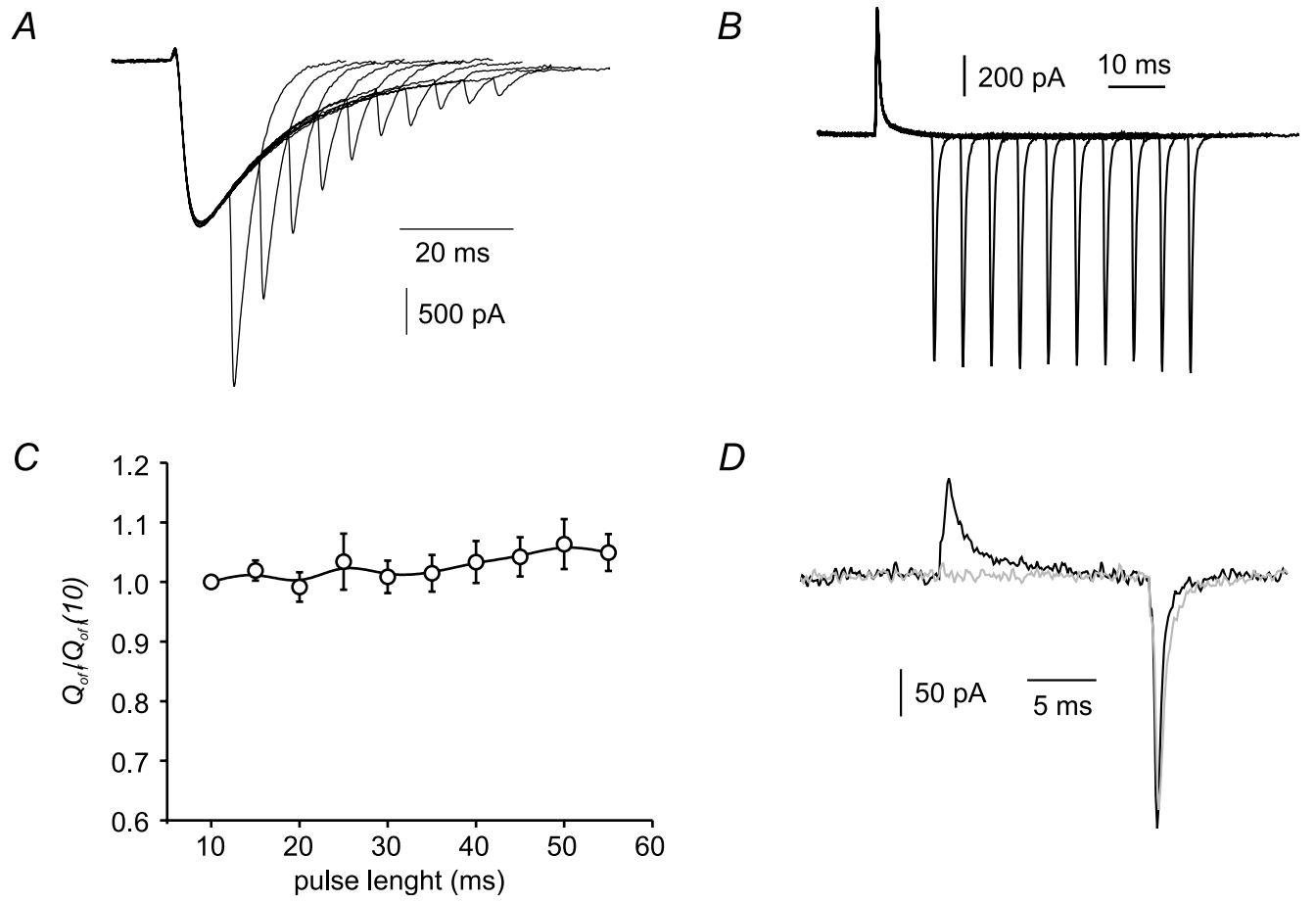

Fig. 4. The gating current of $Ca_v3.1$ channel is not immobilized by prolonged depolarization. A: An example of inward and tail currents recorded in the absence of La^{3+} ions. Currents were activated by depolarizing pulses from the HP of −100 mV to −20 mV (peak of current–voltage relationship) with a length increasing from 10 to 55 ms at a frequency of 0.2 Hz. B: Charge movement was recorded in the presence of 1 mM La^{3+}. Gating current was activated by the same voltage protocol as in panel (A). C: Q_{off}s evaluated at the end of each individual pulse in the panel (B) were normalized to the Q_{off} measured at the end of 10 ms long pulse, averaged and plotted against the pulse length. D: Charge movement was recorded in the presence of 1 mM La^{3+} during 15 ms long depolarizing pulse to −20 mV with (gray line) or without (black line) 5 s long conditioning prepulse to 0 mV.

half-maximal activation voltages ([25] and this paper). In parallel to $Ca_v2.3$ channel, the component with more negative activation has also steeper slope. While transition of 30% of gating charge is sufficient for activation of 68% of the T-type calcium current, transition of the remaining 70% of the charge corresponds to activation of about 32% of the current. A potential explanation for this relative unusual values is that the channel opens before each of the four S4 segment has moved to the open conformation.

The pore region controlling the selectivity and permeation of T-type calcium channels contains two glutamates and two aspartate residues (EEDD), in contrast to four glutamates (EEEE) in all HVA calcium channels. Studies of mutants of these pore residues support the notion that the difference in these pore residues contributes to the voltage dependence of channel opening [31]. Replacement of the pore aspartates with glutamates displaced the activation curves towards positive voltages and enhanced slope values making the voltage dependence of current activation of the mutated T-type channel quantitatively similar to that of HVA calcium channels.

Alternatively, it is possible that even evaluation of channel activation from tail current amplitudes underestimates the number of activated channels, because a very fast inactivation process takes place during the 2 ms long depolarization to high membrane potential. This possibility is supported by the finding that activation of $Ca_v3.3$ channel, a channel with slower activation and inactivation kinetics than the $Ca_v3.1$ channel, continues to increase even above membrane potential of +100 mV [26]. Obviously, further studies are needed to elucidate the connection between gating and activation of T-type channels.

4.3. Lack of immobilization of $Ca_v3.1$ channel

Inactivation of HVA calcium channels is a complex process relying on several structural determinants including pore-forming transmembrane segments and loops, intracellular domain linkers and the carboxyl terminus [32]. Immobilization of charge movement coupled to voltage-dependent channel inactivation was reported for native L-type calcium channel [33] and for expressed $Ca_v2.2$ [16]. Structural determinants and molecular processes underlying LVA channel inactivation are largely unknown. Serrano and coauthors [34] proposed that the decay of current during a depolarizing pulse represents a mixture of voltage-dependent deactivation and voltage-independent inactivation. Here, we have shown that the process by which the depolarizing pulse transfers the $Ca_v3.1$

channel into the non-conducting state does not result in a restriction of the movement of charged parts of the channel. Long depolarizations abolished Q_{on}, but did not affect Q_{off}. This observation is in line with both observations of Burgess and coauthors [35] and Serrano's model [34]. A voltage-independent inactivation process would not involve interaction with the channels voltage sensor and therefore will not result in immobilization of the OFF-charge movement.

Acknowledgements: Supported by DFG (N.K. and F.H.) and Volkswagen Stiftung (L.L.).

References

[1] Hofmann, F., Lacinová, L'. and Klugbauer, N. (1999) Rev. Physiol. Biochem. Pharmacol. 139, 33–87.
[2] Yang, N. and George Jr., A.L. (1996) Neuron 16, 113–122.
[3] Yellen, G. (1998) Q. Rev. Biophys. 31, 239–295.
[4] Horn, R. (2000) Neuron 25, 511–514.
[5] Armstrong, C.M. and Bezanilla, F. (1977) J. Gen. Physiol. 70, 567–590.
[6] Kühn, F.J.P. and Greeff, N.G. (1999) J. Gen. Physiol. 114, 167–183.
[7] Chameau, P., Bournaud, R. and Shimahara, T. (1995) Neurosci. Lett. 201, 159–162.
[8] Bean, B.P. and Rios, E. (1989) J. Gen. Physiol. 94, 65–93.
[9] Shirokov, R., Levis, R., Shirokova, N. and Rios, E. (1992) J. Gen. Physiol. 99, 863–895.
[10] Adams, B.A., Tanabe, T., Mikami, A., Numa, S. and Beam, K.G. (1990) Nature 346, 569–572.
[11] Wang, Z.M., Messi, L. and Delbono, O. (1999) Biophys. J. 77, 2709–2716.
[12] Kamp, T.J., Pérez-García, M.T. and Marban, E. (1996) J. Physiol. 492, 89–96.
[13] Bangalore, R., Mehrke, G., Gingrich, K., Hofmann, F. and Kass, R.S. (1996) Am. J. Physiol. 270, H1521–H1528.
[14] Shirokov, R., Ferreira, G., Yi, J. and Rios, E. (1998) J. Gen. Physiol. 111, 807–823.
[15] Jones, L.P., Patil, P.G., Snutch, T.P. and Yue, D.T. (1997) J. Physiol. 498, 601–610.
[16] Jones, L.P., DeMaria, C.D. and Yue, D.T. (1999) Biophys. J. 76, 2530–2552.
[17] Shirokov, R. (1999) J. Physiol. 518, 697–703.
[18] Olcese, R., Neely, A., Qin, N., Wei, X., Birnbaumer, L. and Stefani, E. (1996) J. Physiol. 497, 675–686.
[19] Jones, L.P., Wei, S.K. and Yue, D.T. (1998) J. Gen. Physiol. 112, 125–143.
[20] Qin, N., Olcese, R., Stefani, E. and Birnbaumer, L. (1998) Am. J. Physiol. 274, C1324–C1331.
[21] Nilius, B., Hess, P., Lansman, J.B. and Tsien, R.W. (1985) Nature 316, 443–446.
[22] Perez-Reyes, E. (1998) J. Bioenerg. Biomembr. 30, 313–318.
[23] Klugbauer, N., Marais, E., Lacinová, L'. and Hofmann, F. (1999) Pflug. Arch. 437, 710–715.
[24] Lacinová, L'., Klugbauer, N. and Hofmann, F. (2000) Neuropharmacology 39, 1254–1266.
[25] Monteil, A., Chemin, J., Bourinet, E., Mennessier, G., Lory, P. and Nargeot, J. (2000) J. Biol. Chem. 275, 6090–6100.
[26] Gomora, J.C., Murbatián, J., Arias, J.M., Lee, J.H. and Perez-Reyes, E. (2002) Biophys. J. 83, 229–241.
[27] Josephson, I.R. (1997) Pflug. Arch. 433, 321–329.
[28] Neely, A., Wei, X., Olcese, R., Birnbaumer, L. and Stefani, E. (1993) Science 262, 575–578.
[29] Meir, A. and Dolphin, A.C. (1998) Neuron 20, 341–351.
[30] Bourinet, E., Zamponi, G.W., Stea, A., Soong, T.W., Lewis, B.A., Jones, L.P., Yue, D.T. and Snutch, T.P. (1996) J. Neurosci. 16, 4983–4993.
[31] Talavera, K., Staes, M., Janssens, A., Klugbauer, N., Droogmans, G., Hofmann, F. and Nilius, B. (2001) J. Biol. Chem. 276, 45628–45635.
[32] Hering, S., Berjukow, S., Sokolov, S., Marksteiner, R., Weiss, R.G., Kraus, R. and Timin, E.N. (2000) J. Physiol. 528, 237–249.
[33] Hadley, R.W. and Lederer, W.J. (1991) J. Gen. Physiol. 98, 265–285.
[34] Serrano, J.R., Perez-Reyes, E. and Jones, S.W. (1999) J. Gen. Physiol. 114, 185–201.
[35] Burgess, D.E., Crawford, O., Delisle, B.P. and Satin, J. (2002) Biophys. J. 82, 1894–1906.